

## Self-organized superlattice patterns with two slightly differing wave numbers

E. Große Westhoff, R. Herrero,\* T. Ackemann, and W. Lange

*Institut für Angewandte Physik, Westfälische Wilhelms-Universität Münster, Corrensstrasse 2/4, D-48149 Münster, Germany*

(Received 31 May 2002; revised manuscript received 16 December 2002; published 19 February 2003)

We report on the observation of superlattices that occur spontaneously in a nonlinear optical system with  $O(2)$  symmetry. A secondary bifurcation from hexagons yields patterns formed by twelve wave vectors. Besides irregular patterns these may either be quasiperiodic patterns or superlattices built from two classes of wave vectors differing slightly in their length. Both classes of wave vectors stem from only one pattern-forming instability. The wave vectors fit on a hexagonal or a square grid. In the former case the set of wave vectors can be decomposed into two hexagonal triads, whereas in the case of the square grid squeezed triads occur.

DOI: 10.1103/PhysRevE.67.025203

PACS number(s): 89.75.Kd, 42.65.Sf, 47.54.+r

Spatially extended nonlinear dissipative systems are capable of generating a wide variety of patterns. Commonly the uniform state of the pattern forming system is unstable against periodic perturbations with a well defined critical wave number  $k_c$  [1]. The superposition of  $n$  wave vectors that are equally distributed on a circle of radius  $k_c$  yields simple periodic (stripes, squares, hexagons for  $n=2,4,6$ ) and quasiperiodic structures ( $n>6$ ) [2,3]. The latter are not periodic since their  $n$ -fold rotational symmetry is not compatible with the translational symmetry.

A quasiperiodic pattern can be converted into a periodic one by varying the angles between the wave vectors and/or the wave numbers in order to break the high rotational symmetry. The new structure is periodic if and only if the wave vectors lie on a periodic grid. For the hexagonal and the square grid, Dionne and Golubitsky analyzed the possible planforms and predicted stability for some *complex periodic* structures [4]. These patterns contain two different length scales and represent *superlattices* [5]. Complex periodic patterns have been observed in systems with broken rotational symmetry [6,7] and in recent experiments in which *two* instabilities are present simultaneously [8,9].

We report the observation of superlattices which belong to a new class of complex structures. They are built from wave vectors whose lengths differ just slightly. All of them stem from the *same* instability [10] and rely on the simple fact that far above threshold a band of wave numbers is unstable.

The experiment (cf., Fig. 1) is based on the *single feed-back mirror arrangement*, which is an archetypal system for optical pattern formation [11]. We irradiate sodium vapor with a circularly polarized Gaussian beam (beam waist  $w_0 = 1.5$  mm) which is tuned near to the sodium  $D_1$  line [12]. The transmitted light is fed back into the medium by a plane mirror (reflectivity  $R=0.92$ ) placed at a distance  $d=45 \cdot \cdot \cdot 90$  mm behind the medium. Due to the insertion of a quarter wave plate between the cell and the mirror, the polarization components counterpropagating in the medium have opposite helicity [13]. A weak longitudinal magnetic field is ap-

plied in order to define the axis of quantization. The intensity distributions of the near field and the far field, which corresponds to the Fourier transform of the former, are monitored with two CCD cameras and are recorded simultaneously.

The most important control parameters in the experiment are the input power and the detuning from the atomic resonance. The parameter space can be roughly divided into seven regions as depicted in Fig. 2. Typically, for increasing input power the homogeneous state (region I) bifurcates to hexagonal patterns (region II), which give way to quasipatterns in region III as discussed in [3].

For higher input power (region IV) we observe a number of different seemingly complex patterns (cf., e.g., Fig. 3). In order to work out the difference between the new patterns and quasipatterns, we analyze them in Fourier space [cf., Figs. 3(b),3(d),3(f),3(h)]. All patterns are built by twelve wave vectors. In the case of the twelvefold quasipattern [cf., Figs. 3(a),3(b)] the Fourier components lie regularly spaced on a ring within the accuracy of the experiment. In other patterns wave numbers differ by up to 10%. Whereas there is no apparent regularity in the pattern displayed in Figs. 3(c),3(d), the Fourier components are arranged in groups of three along approximately straight lines in Figs. 3(f),3(h). This rearrangement results in a sixfold [cf., Fig. 3(f)] and fourfold [cf., Fig. 3(h)] rotational symmetry of the Fourier spectrum that is compatible with spatial periodicity.

We remark that in region IV all patterns described alternate in an irregular way on a time scale of milliseconds for nominally constant parameters. This hints at the existence of multistability with noise induced transitions between different stationary patterns. In the following we will characterize the properties of the new patterns in more detail in parameter regions in which a single type of pattern occurs. In these

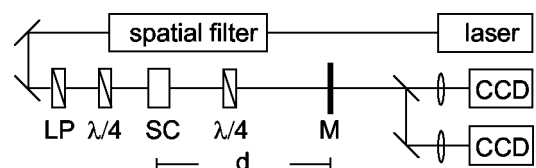


FIG. 1. Schematic experimental setup. LP, linear polarizer;  $\lambda/4$ , quarter-wave plate; SC, sodium cell; M, feedback mirror; CCD, charge coupled camera device.

\*Permanent address: Departament de Física i Enginyeria Nuclear, Universitat Politècnica de Catalunya, c/Comte Urgell 187, E-08036, Barcelona, Spain.

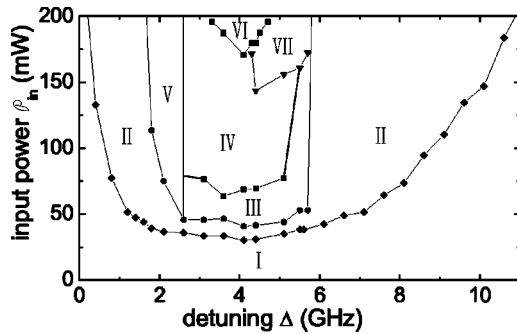


FIG. 2. Schematic bifurcation diagram of dependence on the detuning from the sodium  $D_1$  line and the input power. Parameters: nitrogen buffer gas pressure  $p_{N_2}=200$  hPa, sodium cell temperature  $T=318$  °C, distance between the sodium cell and the feedback mirror  $d=88$  mm, reflectivity of the feedback mirror  $R=92\%$ . The lines have been added to guide the eyes and to roughly separate the regions of different patterns, which are: I, homogeneous state; II, hexagons; III, quasipatterns; IV, multistability; V, SiH+SiH; VI, chessboards; VII, walls. For mirror distances lower than used here the structure  $AS_{2,1}+SiS$  dominates the pattern formation in region IV. A detailed description is given in the text.

regions the patterns are stationary except for slow rotation and drift with varying velocity and direction as expected in a weakly confined system with  $O(2)$  symmetry. The structure with a sixfold far-field pattern [cf., Fig. 3(f)] is monostable within region V in Fig. 2. In this case the far field can be interpreted as a superposition of a hexagonal triad built from wave vectors of the length  $k_1$ , and a second triad with a slightly larger wave number  $k_2$ , which is rotated by an angle of 30 degrees with respect to the former one [cf., Fig. 4(a)].

At the threshold of pattern formation a hexagonal pattern (first triad  $k_1$ ) is observed. For increasing input power the wave number  $k_1$  of the first triad decreases. At about 80% above threshold a second triad with a significantly smaller amplitude appears. Its wave number  $k_2$  is approximately the wave number of the hexagonal pattern at threshold. The ratio  $k_2/k_1$  increases for increasing input power and is 1.120 for the highest accessible input power with a standard deviation of 0.010. This is reasonably close to the ratio  $2/\sqrt{3}\approx 1.155$  for a sixfold superlattice constructed by the superposition of two hexagonal patterns (simple hexagons, SiH according to Fig. 4(a)). In generalization of the notation in Ref. [4] we call this superlattice SiH+SiH. Due to the limited size of the observed patterns the width of the Fourier components (half width at half maximum) is about 5% of their wave number. Therefore, at least within the limited area of pattern formation in the Gaussian beam, an exact correspondence is not necessary to obtain the complex periodicity that can be seen in Fig. 5(a). Some of the minima in the transmitted intensity are slightly elongated and form the centers of squeezed hexagonal cells, which define the new periodicity length and the new symmetry ( $D_2$ ).

For low mirror distances and sufficiently high input power, predominantly patterns of the type depicted in Figs. 3(g),3(h) and 5(c),3(d) are observed. Their far field is formed from eight wave vectors of the same length  $k_2$ , which build a square superlattice [cf., the Fourier components on the

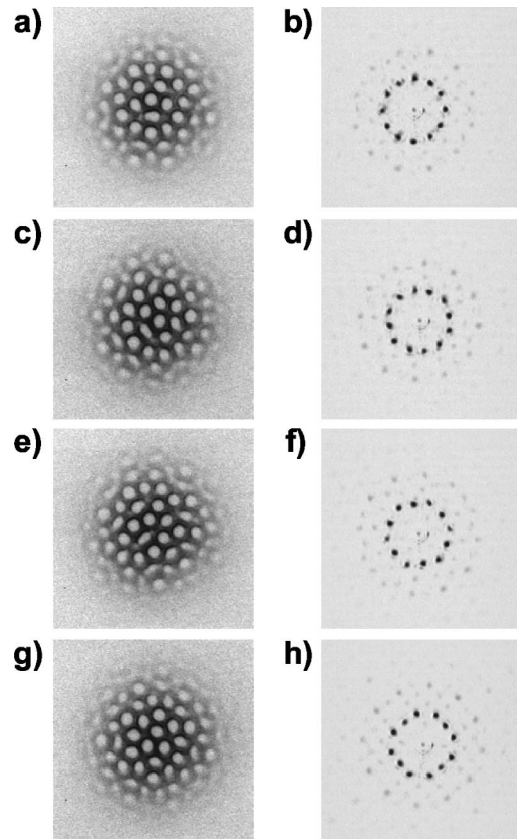


FIG. 3. Experimentally observed near-field (a),(c),(e),(g) and far-field (b),(d),(f),(h) intensity distributions of the transmitted beam for nominal constant parameters, which are given in Fig. 2. The input power is  $P_{in}=113$  mW and the detuning from the sodium  $D_1$  line is  $\Delta=3.6$  GHz.

circle in Fig. 4(b); see also Ref. [4]], and four additional wave vectors of slightly smaller length  $k_1$ , which build a simple square pattern. The ratio between the different wave numbers [cf., Fig. 5(d)] is  $k_2/k_1=1.093$  with a standard deviation of 0.005. This ratio is close to the one expected for the ideal superstructure ( $\sqrt{5}/2\approx 1.118$ ), in that all Fourier components fit on the same square grid. Since the corresponding near-field intensity distribution [cf., Fig. 5(c)] displays a fourfold rotational symmetry but no reflection symmetry, this structure belongs to the symmetry class  $D_4^-$  [4]. This superlattice can be interpreted as a combination ( $AS_{2,1}+SiS$ ) of an antisquare  $AS_{2,1}$  and a simple square (SiS) in the notation of [4].

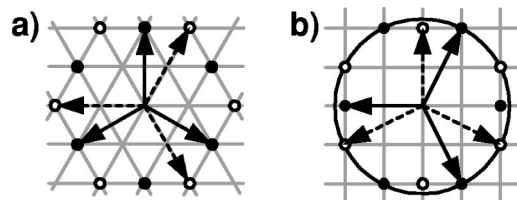


FIG. 4. Schematic Fourier spectrum of two superlattices with (a) sixfold rotational symmetry (SiH+SiH) and (b) fourfold rotational symmetry ( $AS_{2,1}+SiS$  or  $SuS_{2,1}+SiS$ ). The arrows indicate the composition of the patterns by two triads.

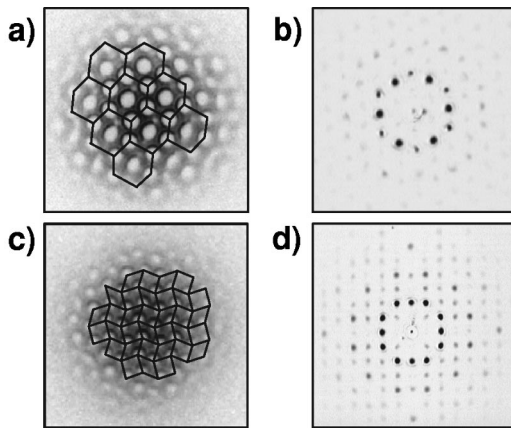


FIG. 5. Near (a),(c) and far (b),(d) -field intensity distribution of superlattice patterns. Parameters: (a),(b) as in Fig. 2 but  $\mathcal{P}_{in} = 182$  mW and  $\Delta = 2.1$  GHz; (c),(d)  $p_{N_2} = 200$  hPa,  $T = 318$  °C,  $\Delta = 4.8$  GHz,  $d = 48$  mm,  $\mathcal{P}_{in} = 162$  mW for (c),(d). Lines are added to the near-field patterns in order to guide the eye along the grid of the superlattices.

The presence of the symmetry  $D_4^-$  excludes the combination (SuS<sub>2,1</sub> + SiS) of a supersquare SuS<sub>2,1</sub> and a simple square, which has the same Fourier power spectrum.

In the parameter regions VI and VII in Fig. 2 we observe squares and stripes with very steep edges, respectively. In the corresponding far-field images the higher harmonics are very strongly excited. In order to distinguish them from ordinary stripes and squares, which do not possess these steep gradients, we call them *walls* and *chessboards*. A detailed discussion of the properties of these patterns cannot be given in this letter, but we mention that chessboardlike patterns have been predicted in optics to occur due to mode coupling between different active instability regions (interballoon coupling [14,15]). In addition, patterns phenomenologically similar to chessboard patterns seem to occur in a single-mirror setup with a photorefractive medium [16].

In fact the linear stability analysis of the microscopic model given in [13] shows a sequence of multiple instability regions that is typical for the single feedback mirror arrangement [11]. For increasing input power the homogeneous steady state initially becomes unstable against periodic perturbations which belong to the instability region with the smallest wave numbers, since that one has the lowest threshold. For higher input power two more instability regions can be activated within the experimentally accessible parameter range. There are indications that these are of importance in the formation of the walls and chessboards.

Numerical simulations, based on the microscopic model given in [13], reproduce the occurrence of the stationary complex periodic patterns in a pump beam with a Gaussian profile. As in the experiment the ratio between the wave numbers is slightly smaller than the values, which are expected for a perfect superlattice on an infinite domain. They are  $1.08 \pm 0.01$  and  $1.09 \pm 0.01$  instead of  $2/\sqrt{3}$  and  $\sqrt{5}/2$ , respectively. In order to check for possible consequences of the inhomogeneous input profile on pattern selection, simulations with a plane wave input beam and periodic boundary

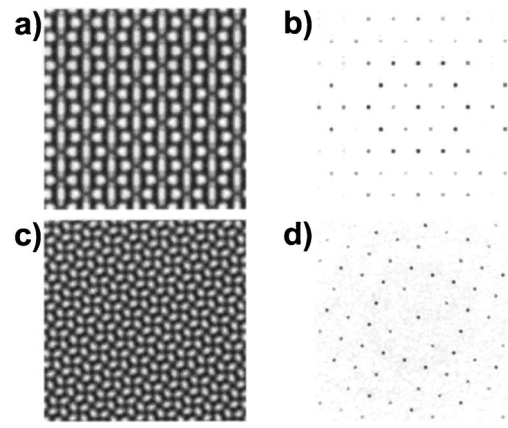


FIG. 6. Intensities of the transmitted near field (a),(c) and far field (b),(d) calculated in numerical simulation with periodic boundary conditions and a plane wave input beam. Parameters:  $d = 88$  mm,  $R = 0.915$ ,  $N = 7.3 \times 10^{18}$  m<sup>-3</sup>,  $D = 356.3 \times 10^{-6}$  m<sup>2</sup>/s,  $\Gamma_2 = 6.83 \times 10^9$  s<sup>-1</sup>,  $L = 15$  mm. Furthermore, in (a),(b)  $\Delta = 2.2$  GHz,  $P_0 = 10^6$  s<sup>-1</sup>; and in (c),(d)  $\Delta = 4.2$  GHz,  $P_0 = 4 \times 10^5$  s<sup>-1</sup>.

conditions were also performed. Figure 6(a) displays the results of a numerical simulation for small detuning ( $\Delta = 2.2$  GHz), in which a hexagonal pattern is used as the initial condition. The intensity of the transmitted field displays the periodic repetition of the same basic structure as the experimental picture in Fig. 5(a), which is an elongated minimum surrounded by six deeper minima building a squeezed hexagon. The far field is composed of two hexagonal triads with different wave numbers. The ratio  $q_2/q_1$  between the wave numbers agrees with  $2/\sqrt{3}$  within our numerical resolution. The structure is interpreted as a SiH + SiH superlattice. For larger detuning ( $\Delta = 4.2$  GHz) noise has been chosen as the initial condition. The intensity of the transmitted field in Fig. 6(c) resembles the experimental observation in Fig. 5(c). The ratio of the two different wave numbers displayed in the far field agrees with  $\sqrt{5}/2$  within our numerical resolution. The structure is interpreted as an AS<sub>2,1</sub> + SiS pattern as in the experiment.

We conclude that the selection of superlattices is not due to the boundary conditions, even though the wave-number ratio is slightly squeezed in a Gaussian beam. However, the deviation is so small that in the limited area of the Gaussian beam the patterns appear as a superlattice.

By suppressing the spatial harmonics of the state variable in the calculations it can be shown that these harmonics are not essential in the formation of the superstructures. This implies that the existence of the higher instability regions mentioned above is not a prerequisite of the process. In contrast, in Refs. [7,9] the superlattice patterns contain wave vectors stemming from different instabilities of the homogeneous state [10].

In the microscopic description of the system the inversion symmetry is broken [13]. Therefore, quadratic terms are present in the amplitude equations describing the dynamics of the complex amplitudes of the bifurcating Fourier modes. This quadratic coupling results in a resonant wave-vector interaction (*hexagonal triad*) that is responsible for the for-

mation of hexagons ([1] and references therein) in parameter region II in Fig. 2. We propose that the same resonant wave-vector interaction also stabilizes the observed complex structures. All structures, which are built from twelve Fourier components (parameter regions III, IV, and V in Fig. 2), can be interpreted as a superposition of two triads of fundamental modes. Indeed, the sum of the wave vectors of the corresponding triads is zero within the error produced by discretization. This indicates the stabilization of each triad due to the resonant interaction between active modes. In the case of the superlattice on the square grid the triad is squeezed [Fig. 4(b)]; it might be called a *square triad*.

Coupling terms between modes belonging to different triads will appear in third order of the amplitude equations. Cubic couplings between modes of the *same* wave number are of the form  $A_i|A_j|^2$ , since the resonance condition for four-wave mixing,  $\sum_{i=1}^4 \vec{q}_i = 0$ , cannot be fulfilled otherwise. However, the superstructures *with two slightly different wave numbers* allow for new resonances which introduce couplings of the type  $A_i A_j A_k^*$ . These couplings are phase sensitive. In a preliminary analysis they select the antisquares instead of supersquares. While the role of the phase sensitiv-

ity of the quadratic coupling is well known to be crucial in the formation of hexagons [1] and superlattices [7], the results indicate that phase-sensitive contributions can also be important in cubic order.

Finally, we would like to emphasize that the superlattices discussed here are by no means a phenomenon that seems to be restricted to very special conditions. On the contrary, in the phase diagram of Fig. 2 there is a wide parameter range, where the increase of the input power gives superlattices by a secondary bifurcation, either directly from hexagons or mediated by quasipatterns. It is not at all apparent that this behavior might be specific to the system under study. Indeed, a recent work indicates that a structure with the same wave-vector configuration as the SiH+SiH superlattice is one of the possible structures which might emerge from a generic secondary bifurcation of hexagons [17].

#### ACKNOWLEDGMENTS

We gratefully acknowledge financial support by the Deutsche Forschungsgemeinschaft and the help of D. Rudolph in some of the measurements. We thank L. Gil for sharing the work [17] prior to publication.

- 
- [1] M. C. Cross and P. C. Hohenberg, *Rev. Mod. Phys.* **65**, 851 (1993).
- [2] B. Christiansen, P. Alstrøm, and M. T. Levinsen, *Phys. Rev. Lett.* **68**, 2157 (1992); W. S. Edwards and S. Fauve, *Phys. Rev. E* **47**, R788 (1993).
- [3] R. Herrero *et al.*, *Phys. Rev. Lett.* **82**, 4627 (1999).
- [4] B. Dionne and M. Golubitsky, *ZAMP* **43**, 36 (1992).
- [5] U. Dahmen, *Encyclopedia of Physical Science and Technology* **10**, 319 (1987).
- [6] S. Douady, *J. Fluid Mech.* **221**, 383 (1990).
- [7] E. Pampaloni, S. Residori, S. Soria, and F. T. Arecchi, *Phys. Rev. Lett.* **78**, 1042 (1997).
- [8] A. Kudrolli, B. Pier, and J. P. Gollub, *Physica D* **123**, 99 (1998).
- [9] H. Arbell and J. Fineberg, *Phys. Rev. Lett.* **81**, 4384 (1998); C. Wagner, H. W. Müller, and K. Knorr, *ibid.* **83**, 308 (1999); J. L. Rogers, M. F. Schatz, J. L. Bougie, and J. B. Swift, *ibid.* **84**, 87 (2000); H.-J. Pi, S. Park, J. Lee, and K. Lee, *ibid.* **84**, 5316 (2000); C. Wagner, H. W. Müller, and K. Knorr, *Phys. Rev. E* **62**, R33 (2000).
- [10] In the patterns discussed in Ref. [8] there is only one fundamental wavelength. Nevertheless, the vicinity of a codimension-2 bifurcation point is considered to be important.
- [11] G. D'Alessandro and W. J. Firth, *Phys. Rev. Lett.* **66**, 2597 (1991).
- [12] T. Ackemann, Y. Logvin, A. Heuer, and W. Lange, *Phys. Rev. Lett.* **75**, 3450 (1995).
- [13] A. Aumann *et al.* *J. Opt. B: Quantum Semiclassical Opt.* **1**, 166 (1999).
- [14] M. A. Vorontsov and A. Y. Karpov, *J. Opt. Soc. Am. B* **14**, 34 (1997).
- [15] M. Le Berre, D. Leduc, E. Ressayre, and A. Tallet, *Asian J. Phys.* **7**, 483 (1998).
- [16] M. Schwab *et al.* *Chaos, Solitons Fractals* **10**, 701 (1999).
- [17] C. Pirat, and L. Gil (unpublished).